Lattice modes mediate radiative coupling in metamaterial arrays

Andreas Bitzer[1,2*], Jan Wallauer[1], Hanspeter Helm[1], Hannes Merbold[2], Thomas Feurer[2], and Markus Walther[1*]

[1]*Freiburg Materials Research Center, University of Freiburg, Stefan-Meier-Strasse 21, D-79104 Freiburg, Germany*

[2]*Institute of Applied Physics, University of Bern, Sidlerstr. 5, CH-3012 Bern, Switzerland*

[*]*Corresponding Authors:*

andreas.bitzer@gmail.com

markus.walther@physik.uni-freiburg.de

Abstract: We show that a resonant response with very high quality factors can be achieved in periodic metamaterials by radiatively coupling their structural elements. The coupling is mediated by lattice modes and can be efficiently controlled by tuning the lattice periodicity. Using a recently developed terahertz (THz) near-field imaging technique and conventional far-field spectroscopy together with numerical simulations we pinpoint the underlying mechanisms. In the strong coupling regimes we identify avoided crossings between the plasmonic eigenmodes and the diffractive lattice modes.

OCIS codes: (300.6495) Spectroscopy; (160.3918) Metamaterials.

References and links

1. J. B. Pendry, D. Schurig, and D. R. Smith, "Controlling electromagnetic fields," Science **312**, 1780–1782 (2006).
2. C. M. Soukoulis, S. Linden, and M. Wegener, "Negative refractive index at optical wavelengths," Science **315**, 47–49 (2007).
3. V. M. Shalaev, "Optical negative-index metamaterials," Nat. Photonics **1**, 41–48 (2007).
4. J. B. Pendry, A. J. Holden, D. J. Robbins, and W. J. Stewart, "Magnetism from conductors and enhanced nonlinear phenomena," IEEE Trans. Microwave Theory Tech. **47**, 2075–2084 (1999).
5. D. R. Smith, J. B. Pendry, and M. C. K. Wiltshire, "Metamaterials and negative refractive index," Science **305**, 788–792 (2004).
6. H. T. Chen, W. J. Padilla, J. M. O. Zide, A. C. Gossard, A. J. Taylor, and R. D. Averitt, "Active terahertz metamaterial devices," Nature **444**, 597–600 (2006).
7. H. T. Chen, J. F. O'Hara, A. K. Azad, A. J. Taylor, R. D. Averitt, D. B. Shrekenhamer, and W. J. Padilla, "Experimental demonstration of frequency-agile terahertz metamaterials," Nat. Photonics **2**, 295–298 (2008).
8. R. Singh, C. Rockstuhl, F. Lederer, and W. L. Zhang, "Coupling between a dark and a bright eigenmode in a terahertz metamaterial," Phys. Rev. B **79**, 085111 (2009).
9. N. Liu, S. Kaiser, and H. Giessen, "Magnetoinductive and Electroinductive Coupling in Plasmonic Metamaterial Molecules," Adv. Mater. **20**, 4521–4525 (2008).
10. P. Tassin, L. Zhang, T. Koschny, E. N. Economou, and C. M. Soukoulis, "Low-Loss Metamaterials Based on Classical Electromagnetically Induced Transparency," Phys. Rev. Lett. **102**, 053901 (2009).
11. V. A. Fedotov, M. Rose, S. L. Prosvirnin, N. Papasimakis, and N. I. Zheludev, "Sharp trapped-mode resonances in planar metamaterials with a broken structural symmetry," Phys. Rev. Lett. **99**, 147401 (2007).
12. N. Liu, H. C. Guo, L. W. Fu, S. Kaiser, H. Schweizer, and H. Giessen, "Three-dimensional photonic metamaterials at optical frequencies," Nat. Mater. **7**, 31–37 (2008).
13. N. Liu, L. Langguth, T. Weiss, J. Kästel, M. Fleischhauer, T. Pfau, and H. Giessen, "Plasmonic analogue of electromagnetically induced transparency at the Drude damping limit," Nat. Mater. **8**, 758–762 (2009).

#117867 - $15.00 USD Received 28 Sep 2009; revised 11 Nov 2009; accepted 11 Nov 2009; published 18 Nov 2009

14. F. Hao, P. Nordlander, M. T. Burnett, and S. A. Maier, "Enhanced tunability and linewidth sharpening of plasmon resonances in hybridized metallic ring/disk nanocavities," Phys. Rev. B **76**, 245417 (2007).
15. E. Prodan, C. Radloff, N. J. Halas, and P. Nordlander, "A hybridization model for the plasmon response of complex nanostructures," Science **302**, 419–422 (2003).
16. S. Linden, J. Kuhl, and H. Giessen, "Controlling the interaction between light and gold nanoparticles: Selective suppression of extinction," Phys. Rev. Lett. **86**, 4688–4691 (2001).
17. B. Auguie and W. L. Barnes, "Collective resonances in gold nanoparticle arrays," Phys. Rev. Lett. **101**, 143902 (2008).
18. V. G. Kravets, F. Schedin, and A. N. Grigorenko, "Extremely narrow plasmon resonances based on diffraction coupling of localized plasmons in arrays of metallic nanoparticles," Phys. Rev. Lett. **101**, 087403 (2008).
19. G. Acuna, S. F. Heucke, F. Kuchler, H. T. Chen, A. J. Taylor, and R. Kersting, "Surface plasmons in terahertz metamaterials," Opt. Express **16**, 18745–18751 (2008).
20. A. J. L. Adam, J. M. Brok, M. A. Seo, K. J. Ahn, D. S. Kim, J. H. Kang, Q. H. Park, M. Nagel, and P. C. M. Planken, "Advanced terahertz electric near-field measurements at sub-wavelength diameter metallic apertures," Opt. Express **16**, 7407–7417 (2008).
21. J. R. Knab, A. J. L. Adam, M. Nagel, E. Shaner, M. A. Seo, D. S. Kim, and P. C. M. Planken, "Terahertz Near-Field Vectorial Imaging of Subwavelength Apertures and Aperture Arrays," Opt. Express **17**, 15072–15086 (2009).
22. A. Bitzer and M. Walther, "Terahertz near-field imaging of metallic subwavelength holes and hole arrays," Appl. Phys. Lett. **92**, 231101 (2008).
23. A. Bitzer, H. Merbold, A. Thoman, T. Feurer, H. Helm, and M. Walther, "Terahertz near-field imaging of electric and magnetic resonances of a planar metamaterial," Opt. Express **17**, 3826–3834 (2009).
24. R. W. Wood, "Anomalous Diffraction Gratings," Phys. Rev. **48**, 928–936 (1935).
25. B. E. A. Saleh and M. C. Teich, *Fundamentals of Photonics* (John Wiley & Sons, Inc., New York, 1991).
26. N. Liu, H. C. Guo, L. W. Fu, S. Kaiser, H. Schweizer, and H. Giessen, "Plasmon hybridization in stacked cut-wire metamaterials," Adv. Mater. **19**, 3628–3632 (2007).

1. Introduction

Metamaterials have recently attracted considerable interest due to their potential application for perfect lensing, invisibility cloaking, or as negative refractive index material [1, 2, 3]. These artificially designed media typically consist of periodically arranged metallic structures [4, 5], which show a strong resonant response to an incident electromagnetic field. The ability to customize metamaterials requires control over the strength, linewidth and spectral position of their resonances. For this purpose actively controlable metamaterials have been demonstrated at terahertz frequencies based on the implementation of photo- or electro-active elements [6, 7]. However, their implementation requires advanced processing steps and scaling such devices to higher frequencies has not yet been achieved. Another powerful concept for tailoring metamaterial resonances uses coupling between individual eigenmodes of closely spaced structures such as adjacent [8, 9, 10, 11] or laterally stacked split ring resonators (SRRs) [12] or wires [13]. These studies have been inspired by the demonstration of spectral tunability of localized plasmon resonances in coupled metallic nanostructures where the interaction between the modes of individual nanoparticles gives rise to new hybrid modes [14, 15]. Recently, this concept has been generalized to the coherent interaction between multiple nanostructures arranged in arrays. In these studies efficient control over the plasmonic resonances of metallic nanoparticles has been achieved [16, 17, 18]. It was shown recently that such collective excitations also considerably affect the optical properties of THz metamaterials [19]. Here we study this effect in detail and demonstrate that radiative coupling between the sub-units in a periodic metamaterial is the underlying mechanism. Choosing appropriate lattice geometries a remarkable increase of the quality factors of the metamaterial resonances can be achieved.

2. Plasmonic eigenmodes of an isolated SRR

In order to identify plasmonic resonances in a metamaterial structure without coupling between neighboring elements we first investigate an isolated U-shaped SRR as shown in the inset of

#117867 - $15.00 USD Received 28 Sep 2009; revised 11 Nov 2009; accepted 11 Nov 2009; published 18 Nov 2009

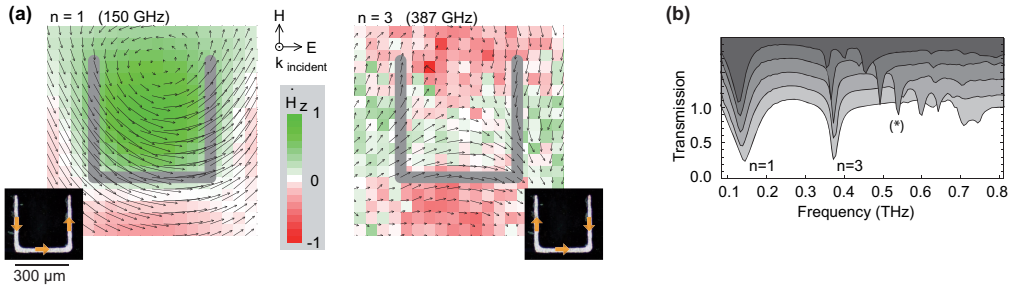

Fig. 1. THz near-field scan (a) of a single SRR at its plasmonic resonances (n=1, n=3) showing the in-plane electric (arrows) and out-of-plane magnetic (color code) near-fields (Media 1). (b) Transmission through rectangular arrays of SRRs with $g_x = 380$ m and $g_y = 380 - 653$ m (bottom to top) (Media 2) showing their fundamental resonances and transmission minima that originate from the excitation of lattice modes (*). The spectra are vertically offset for clarity.

Fig. 1(a). The samples, fabricated by conventional photo-lithography and etching techniques, are 9 m thick copper structures on a 120 m thick PTFE-substrate. Time-domain imaging with pulsed THz radiation offers the unique possibility to measure the electric near-field distribution close to metallic objects with subwavelength spatial resolution [20, 21]. Our recently developed scanning-type THz near-field imaging technique [22, 23] allows to map the electric and magnetic near-fields of the SRR sample at its dominant resonances. Figure 1(a) shows the measured in-plane electric (arrows) and out-of-plane magnetic near-fields (color code) excited on the structures by a normally incident THz-wave linearly polarized along the x-axis. For the chosen polarization the plasmonic eigenmodes are observed whenever the wire length of the unfolded SRR approaches odd multiples of half the wavelength ($l = n \cdot \lambda/2$, $n = 1,3,5,...$). Even eigenmodes are forbidden due to the asymmetry of the electric potential provided by the incident field. The fundamental eigenmode of the SRR (n=1) is observed at 150 GHz and is associated with a circular current oscillating around the ring inducing a magnetic dipole (LC-resonance). The next higher mode observed corresponds to the formation of an electric quadrupole (n=3) with the electric field lines pointing toward and away from the corners of the structure [23]. The directions of the corresponding currents are indicated in the insets. The eigenmodes of the structures are also observed as characteristic transmission minima in the far-field spectra obtained from conventional THz spectroscopy of arrays with different lattice periodicities (from bottom to top: $g_y = 380$ to 653 m) shown in Fig. 1(b).

3. Excitation of lattice modes

In addition to the plasmonic eigenmodes, transmission minima are observed at higher frequencies, labeled by an asterisk in Fig. 1(b). Here, constructive interference of the radiation which is scattered by the periodic lattice causes abrupt changes in transmission due to the so called Wood anomalies [24]. These spectrally shifting lattice modes are clearly distinguishable from the almost stationary plasmonic modes (n=1 and n=3). In a rectangular array lattice modes are formed under the condition:

$$k^2 = i^2 \left(\frac{2\pi}{g_x}\right)^2 + j^2 \left(\frac{2\pi}{g_y}\right)^2, \qquad (1)$$

where $k = \omega/c$ is the wavenumber of the scattered light, c is the speed of light in the surrounding

#117867 - $15.00 USD Received 28 Sep 2009; revised 11 Nov 2009; accepted 11 Nov 2009; published 18 Nov 2009

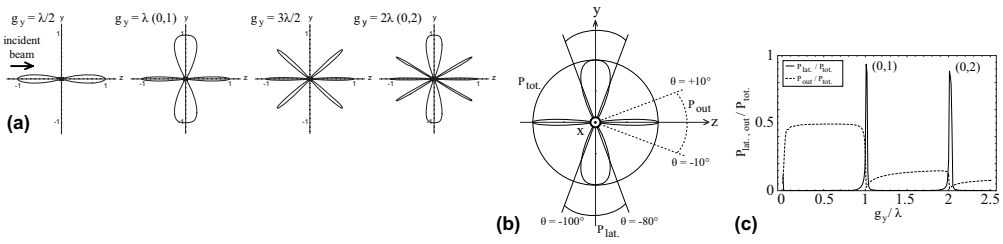

Fig. 2. (a) Far-field intensity distributions of the scattered light calculated for a 1-D array consisting of five isotropic scatterers at different periodicities g_y. The array is oriented along the y-axis and the incident beam propagates in z-direction. (b) Scattering distribution for $g_y = \lambda$. Intensities are integrated over the angular intervals indicated by solid and dashed lines to determine the fractions of light scattered in and out of the sample plane. (c) Integrated intensities as a function of the lattice constant in units of the wavelength.

medium, and (i, j) is a pair of integers defining the diffraction order. Figure 2 (a) shows the angular distribution of the diffracted far-field intensity for different lattice periodicities. The distributions are calculated for five isotropic point scatterers in linear arrangement along the y-axis [25]. The incident light propagates along the z-axis. For $g_y = \lambda/2$ the scattered fields interfere constructively only in the forward and backward directions (zero-order diffraction) and thus radiate into free space. At $g_y = \lambda$ constructive interference also occurs for field components scattered into the sample plane (first diffraction order). This field contribution is coupled to other elements rather than to free space so that its energy gets "trapped" in the array.

By integrating the intensity distributions over an angular interval ($\Delta\Theta = \pm 10^\circ$) for two perpendicular directions as indicated in Fig. 2(b) we determine the fractions of light which are diffracted into the lattice plane and in detector direction, respectively. The part which is scattered into the lattice plane $P_{\text{lattice}}/P_{\text{total}}$ is plotted in Fig. 2(c) as a function of the lattice constant g_y in units of the wavelength λ (solid curve). At the (0,1) and (0,2) diffraction orders two dominant peaks occur. By further increasing the number of participating scatterers the diffraction lobes become narrower and the corresponding peak maxima approach 1. In this case ohmic damping and lattice imperfections are limiting the linewidths of the resonances. The corresponding intensity fraction $P_{\text{out}}/P_{\text{total}}$ which is radiated in detector (forward) direction is indicated by the dashed curve. The lattice excitations are expressed by asymmetric minima with a sharp edge at the low frequency and a broad slope at the high frequency side.

4. Radiative coupling in SRR arrays mediated by lattice modes

In order to study the effect of lattice diffraction on the plasmonic eigenmodes we have fabricated a set of rectangular arrays of SRRs in which the lattice periodicity in y-direction changes in 24 steps from $g_y = 380$ to 1200 m, while the x-periodicity is constant at $g_x = 380$ m. Their transmission has been characterized by a conventional far-field THz time-domain spectrometer and the spectral evolution is plotted in Fig. 3(a) as a function of the reciprocal lattice constant $1/g_y$. In these dispersion diagrams the dotted horizontal lines mark the spectral position of the plasmonic eigenmodes of the individual SRR. The solid lines indicate the various lattice excitations calculated according to Eq. (1). Basically all features expected are observed in the measurements. Of particular interest are the regions where the plasmonic structure and the diffractive lattice modes meet. At the intersection of the n=3 eigenmode with the (0,1) lattice resonance, for example, a pronounced anticrossing indicates strong interaction between the modes. A similar but weaker avoided crossing is observed between the structure resonance n=5

#117867 - $15.00 USD Received 28 Sep 2009; revised 11 Nov 2009; accepted 11 Nov 2009; published 18 Nov 2009

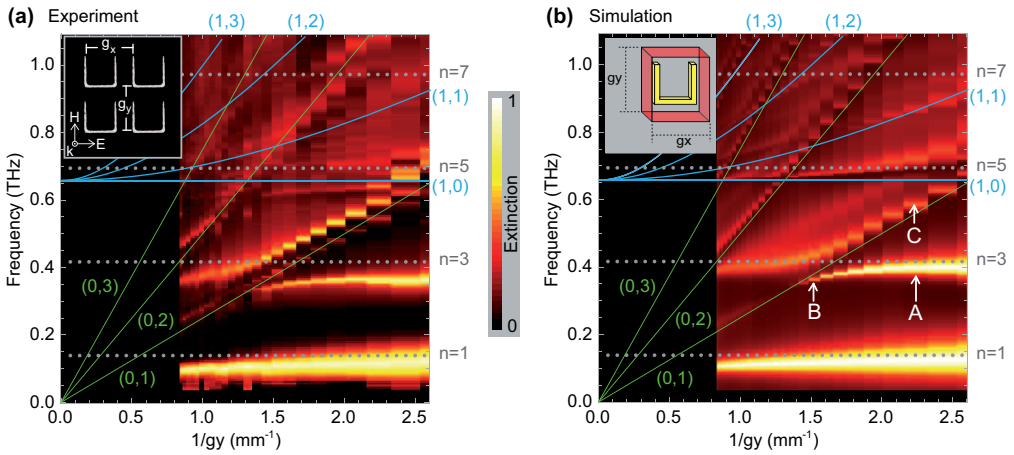

Fig. 3. (a) Dispersion diagram obtained from the measured transmission spectra. In the measurement the lattice constant g_y is changed in steps from 380 to 1200 m while $g_x = 380$ m is constant. Plasmonic structure resonances are indicated by dotted lines (gray), and lattice modes by solid lines (green, blue). (b) Dispersion diagram of the simulated spectra. A and B mark weak and strong radiative coupling regimes for the n=3 mode and C a pure lattice mode. The inset shows the simulation volume with embedded SRR-structure and periodic boundaries on the sides (red). (color online)

and the (0,2) lattice mode. A remarkable observations is that the structure modes significantly sharpen as the lattice modes approach the resonances.

Our experimental observations are confirmed with numerical simulations using a commercial finite-element program package (COMSOL Multiphysics). Here a single SRR has been placed in the center of a 3-D simulation volume with periodic boundaries on the four sides as shown in the inset of Fig. 3(b). Plane waves were incident from the front and the transmitted field has been sampled on the back. Our numerical model reproduces the experimental data (Fig. 3(a)) correctly, in particular the anti-crossing and the line-width sharpening of the n=3 mode. In addition, higher order diffraction modes can be identified which could not be observed in the experimentally recorded spectra due to the limited S/N-ratio.

As discussed above, at the crossing points one of the diffraction lobes radiates into the sample plane, supporting interaction between the individual resonators through radiative coupling. The sharpening of the plasmonic line shape is due to the fact that in case of radiative coupling parts of the diffracted field are trapped in the lattice and couples to neighboring structures. Therefore, radiative damping is significantly reduced leading to a higher quality factor of the corresponding resonance and an associated narrower linewidth. The strong coupling of the plasmonic eigenmodes via the diffractive lattice modes eventually results in an anti-crossing of their energy bands. The maximum energy splitting observed in our experiment is on the order of ~ 78 GHz (0.32 meV) for a lattice constant of $g_y = 708$ m. We note, that in stark contrast to capacitive or conductive coupling which requires closely spaced structures [8, 26], radiative coupling is mediated by long-range lattice modes.

Due to the tight THz focus our near-field imaging setup limits coherent sample excitation to only a small section of an array (on the order of 3x3 structures) which is not sufficient to efficiently excite long-range lattice modes. Therefore, we use the simulations to investigate the influence of radiative coupling on the SRR-modes in the near-field. In Fig. 4(a) the average in-plane power flow is plotted in a plane 20 m behind the structure. The plots show the n=3

#117867 - $15.00 USD Received 28 Sep 2009; revised 11 Nov 2009; accepted 11 Nov 2009; published 18 Nov 2009

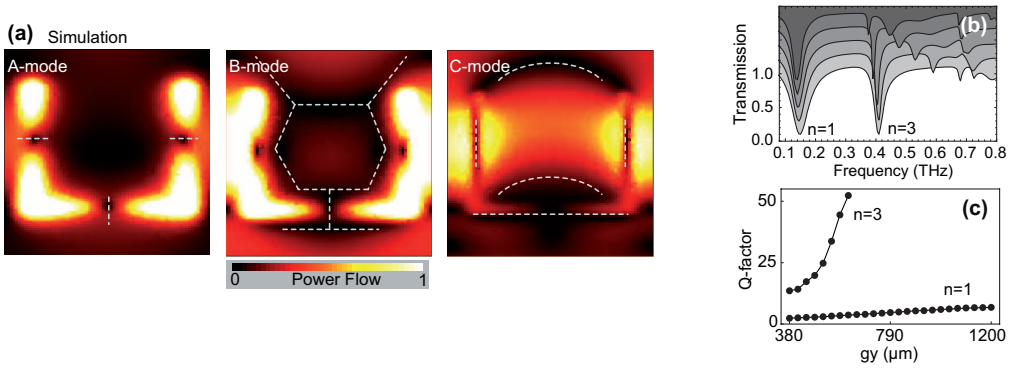

Fig. 4. (a) Average in-plane power flow shown for weak (A-mode) and strong radiative coupling (B-mode) as well as for the (0,1) lattice mode (C-mode). (b) Evolution of the simulated transmission spectrum from the weak to the strong coupling regime (A to B see Fig. 3(c)) (Media 3). The spectra are vertically offset for clarity. (c) Corresponding Q-factors of the plasmonic resonances. (color online)

plasmonic (A-mode), the coupled mode (B-mode), and the (0,1)-lattice mode (C-mode), as marked in Fig. 3(c). In the weak coupling regime (A-mode) maxima at the four corners and pronounced minima (dashed lines) in-between indicate the purely quadrupole-like character of the plasmonic structure resonance. As extracted from our simulation the heat dissipation in the metal skin is 1.4 % of the total power loss as a result of ohmic damping. In case of coupling (B-mode) mode mixing occurs. The plasmonic quadrupole pattern gets superimposed by field contributions from the lattice mode. The heat dissipation is 2.4 %, more than for the uncoupled plasmonic eigenmode (A-mode) since the engergy gets trapped in the array and thus the currents are amplified. In contrast, for the pure lattice mode (C-mode) the energy is stored mainly in the non-metallic regions. Power minima along the SRR-surface indicate weak current flow. This is also reflected in the reduced heat dissipation (<0.002 %).

In Fig. 4(b) the spectral evolution from the weak to the strong coupling regime (A to B) is shown for selected lattice periodicities ($g_y = 380$ to 653 m). The sharpening of the linewidth of the plasmonic resonances is quantified in terms of their quality factors $Q = \nu/\Delta\nu$ shown in Fig. 4(c). Quality factors as high as 50 are achieved close to the crossing points for the n=3 resonance, which corresponds to an improvement by at least 1 order of magnitude. This Q-factor achieved with a conventional SRR design is comparable to that of asymmetric split ring structures which have been recently reported to reach exceptionally high quality factors [11].

5. Conclusion

In summary, we have shown that changing the lattice periodicity in metamaterial arrays allows to control coupling between the "meta-atoms" via their radiated fields. For appropriate chosen lattice periodicities strong radiative coupling causes avoided crossings in the transmission spectrum and leads to large quality factors of the resonances. Our approach provides a novel route to shape resonances in metamaterials and is scalable in frequency. These findings pave the way for optimized design of metamaterials.

Acknowledgment

Financial support by the Deutsche Forschungsgemeinschaft (DFG), grant WA 2641/3, and the Schweizerischer Nationalfonds (SNF), grant 200020-119934, is gratefully acknowledged.

#117867 - $15.00 USD Received 28 Sep 2009; revised 11 Nov 2009; accepted 11 Nov 2009; published 18 Nov 2009